Deformation Simulation in an Elastomechanical Ventricular Model

MB Mohr[1], G Seemann[1], FB Sachse[2], O Dössel[1]

[1]Institute of Biomedical Engineering, University Karlsruhe (TH), Germany
[2]Nora Eccles Harrison Cardiovascular Research and Training Institute, University of Utah, USA

Abstract

The heart's pumping function is dependent on the vitality of the heart muscle, which is mostly composed of contractile cells, so-called myocytes. The orientation of these myocytes throughout the muscle results in a unique profile of contraction allowing the pumping process to be possible. Knowledge of arrangement and physiological properties of these cells permits the creation of realistic computer models. Simulations with computer models can be used e. g. for pre-interventional planing and for educational purposes. The utilized elastomechanical model is based on a spring mass system enhanced by continuum mechanics based methods. A truncated ellipsoid is chosen to represent a ventricle. Three simulation scenarios were chosen, in which parameters varied to simulate behavior of normal, dilated, and necrotic tissue. The results of these three studies are discussed with focus on change of inner ventricular volume, tissue volume, and suitability of the elastomechanical ventricular model for pathologic tissue modeling. As deformation results show, the presented model is able to reconstruct pathologic and non-pathologic mechanical properties of myocardium.

1. Introduction

The heart's pumping function is determined by myocytes and their orientation throughout the muscle. Knowledge of physiological properties and functionality of myocytes enables the design of appropriate computer models. Simulations with an anatomically based model allow to evaluate surgical procedures and can be used for pre-interventional planing as well as for educational purposes.

In this work a ventricle model was created as a truncated half ellipsoid. The model held anatomical and physical properties such as fiber orientation and electrical conductivity. The simulation process can be differentiated into electrophysiology, excitation propagation, tension development, and deformation. The utilized mechanical model was based on a hybrid model consisting of a spring mass system extended by continuum mechanical calculations. Simulations with regional changes of tissue characteristics were applied to model behavior of normal, necrotic, and dilated tissue. Therefore, this work is focused on simulations of mechanical deformation of an elastomechanical ventricular model for pathologic scenarios and the resulting mechanical differences.

2. Methods

An elastomechanical ventricular model was represented as a truncated half ellipsoid. Due to the high computation cost, the studies were done using a model of a smaller-sized ventricle not representing an anatomically correct size. It was rendered in a $26 \times 26 \times 33$ cubic voxel lattice with a voxel edge length of $0.2\ mm$. Each voxel held physical properties necessary for electromechanical simulations. A realistic fiber orientation varying from epi- to endocardium from $-75\,^\circ$ to $75\,^\circ$ was implemented (Fig. 1). Electrophysiological simulations were carried out by applying a model of Noble et al. [1]. The bidomain model was used for reconstruction excitation propagation through the ventricle [2]. The initial electrical stimulus was set at the apex of the ellipsoid. Electromechanical coupling was implemented via exchange of intracellular concentration of calcium concentration [3] resulting in a

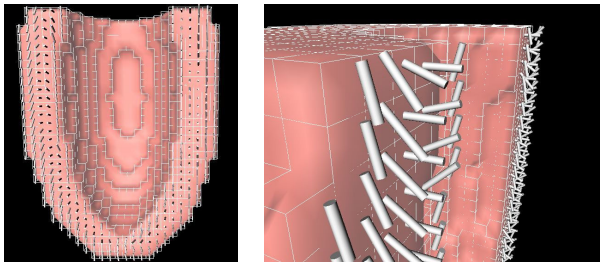

Figure 1. A truncated ellipsoid was rendered in a $26 \times 26 \times 33$ cubic voxel lattice with edge length of $0.2\ mm$. The left figure shows a lateral cut with fiber orientation for each voxel. The right figure displays the upper left corner, where the twist of fiber orientation from endo- to epicardium is visualized with white cylinders.

time course of force development. These simulations were performed prior to deformation simulation.

2.1. Hybrid Deformation Model

The geometry of the truncated half ellipsoid model was the base for the hybrid deformation model [4, 5]. This model is based on a spring mass system proposed by Bourguignon et al. [6] and continuum methods [7, 8, 9]. Each voxel was represented by masses at the voxel corners and several connective springs [4] (Fig. 2). The tissue mass was dispatched with the help of Voronoi region. Springs at the voxel surface, diagonally through the voxel as well as along the voxel edges were used for structural integrity. The fusion model of Miyazaki et al. [10] was implemented for partial spring rigidity. The anisotropy was modeled by three springs in fiber, sheet, and sheet normal direction. In addition a continuum mechanics model of Guccione et al. [11] was implemented, which utilizes an exponential strain energy density function to model passive anisotropic myocardial tissue. Parameters were chosen as described by Sachse [8]. The force generated in fiber direction was translated by linear interpolation to the corner masses. The isovolumetric part of the Mooney-Rivlin strain energy density function was implemented to enhance the incompressibility of tissue [12]. At each time step the forces of springs and the tension created by energy density functions were evaluated and the masses were displaced accordingly. An iterative process was used to find an energetic minimum prior to applying the next time step.

2.2. Simulation Scenarios

Simulation were carried out as follows: The myocardial tension was calculated with a force development model. The force distribution was calculated up to 1000 ms in 50 steps of 2 ms. Deformation simulations were done with all force distributions and lasted until an energetic minimum was established.

A simulation of normal tissue was performed on the truncated ellipsoid. Tissue was set up as vital living tissue with linear springs, Gucciones strain energy density function, and Mooney-Rivlins incompressibility function.

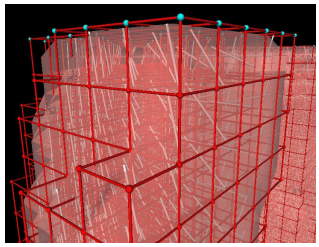

Figure 2. View inside the truncated half ellipsoid. Cylinders at the voxel edges represent structural springs and spheres show mass points at the voxel corners. The cylinders inside display the fiber orientation.

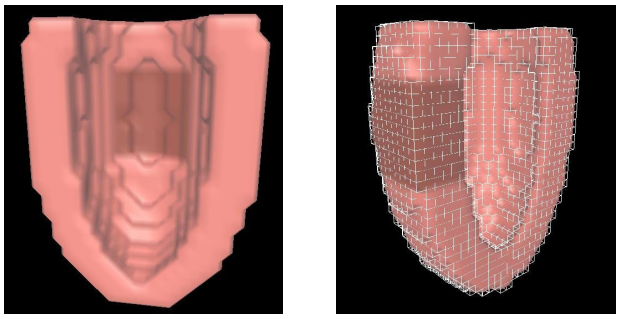

Figure 3. Lateral view of open truncated half ellipsoid. The darker region displays the $8\times9\times10$ voxel patch with pathologic tissue properties. The wireframe denotes undeformed position.

A region of the wall with the size of $8\times9\times10$ voxel was set to either necrotic or dilated tissue (Fig. 3) for the pathologic setups. All parameters described below were found empirically. Pathologic tissue was assumed to be unexcitable and not complying to passive properties of normal tissue. Necrotic tissue was assumed to be stiff. Dilated tissue was assumed to be viscose.

2.2.1. Necrotic Region

The necrotic region was simulated by setting parameters for the $8\times9\times10$ voxel region as follows:

The exponential strain energy density function of Guccione et al. and Mooney-Rivlin was deactivated. Spring parameters for stiffness and damping were reduced to approximately 10% and 40%, respectively. The tissue density was slightly raised to simulate greater inertia. The parameter for the fusion model was increased to enhance rigidity of springs.

2.2.2. Dilated Region

The dilated region was simulated by setting parameters for the $8\times9\times10$ voxel region as follows:

The exponential strain energy density function of Guccione et al. and Mooney-Rivlin was deactivated. Spring parameters were reduced to approx. 5% and damping was turned off. The tissue density was held constant. The rigidity of the fusion model was turned off.

3. Results

Deformation simulations with the described scenarios were conducted. The deformation results are displayed (Fig. 4, 5, 6). The movement of the apex of the half ellipsoid is similar for all three systems (Fig. 4). The

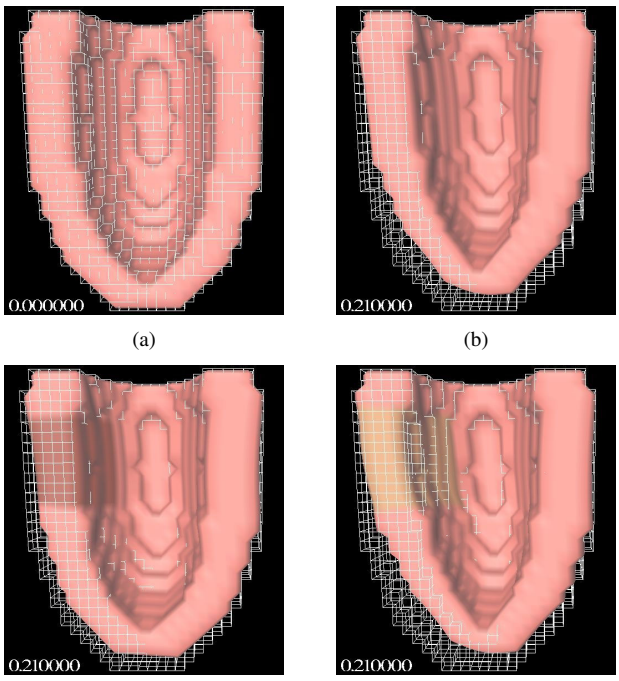

(a) (b) (c) (d)

Figure 4. Lateral view of truncated half ellipsoid. Top row shows normal tissue (a) at rest and (b) at maximal deformation . Lower row depict pathologic tissue simulation at maximal deformation at 0.210 s. The patch of necrotic tissue in dark shade (c) and patch of dilated tissue in light shade (d). The white wireframe denotes half ellipsoid without deformation.

necrotic simulation (Fig. 4 c) shows in the lower half of the ventricle less contraction compared to simulations done in normal tissue.

For normal tissue, the wall at the patch shows a light curvature towards the inside of the ventricle, whereas the necrotic patch forms a straight line, and the dilated wall bends lightly towards the outside of the ventricle.

The view from the apex upwards displays the torsion for each simulation (Fig. 5). Both simulations of pathological conditions show a reduced torsion as seen in figure 5. Further studies need to be done to determine exact differences in torsion of these simulations.

A comparison between maximal deformation of normal and pathologic tissue is visualized in figure 6. The left column depicts necrotic tissue and the right column represents dilated tissue.

Simulations of necrotic tissue revealed a reduced torsion within the normal tissue below the pathologic area compared to simulations of normal tissue as the surface exceeds the wireframe (Fig. 6 a). The symmetric proportion within the necrotic model remains constant, as at the opposite side surface rendering is behind the wireframe (Fig. 6 c). The necrotic patch keeps its width compared to a thickened wall of the normal tissue,

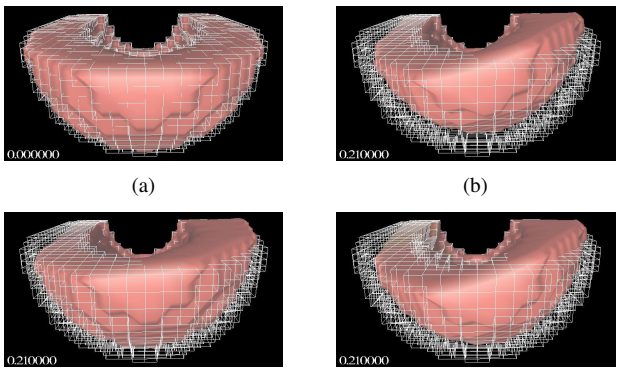

(a) (b) (c) (d)

Figure 5. Basal view of truncated half ellipsoid. Top row shows the normal tissue and lower row depicts pathologic tissue simulation (left necrotic, right dilated) at maximal deformation at 0.210 s. as in figure 4.

which denotes the wireframe in front of surface rendering (Fig. 6 a, 6 e). The apex upward movement is diminished (Fig. 6 c).

The torsion within the dilated model is stronger on the side of the necrotic area than within normal tissue. However, symmetry is lost as the opposite side of the patch does not exceed the normal tissue (wireframe in front of surface rendering)(Fig. 6 b, 6 f). Again, the apex upward movement is diminished (Fig. 6 d). The tissue at the patch is deformed outward (Fig. 6 f).

For each simulation the cavity volume and tissue volume was calculated and plotted at each time step (Fig. 7). The graph of normalized cavity volume shows the normalized filling volume of the ventricle model throughout the progression of a simulation sequence (Fig. 7). The simulations of pathological conditions showed a reduced volume displacement by 7% for necrotic tissue and by 3% for dilated tissue compared to normal conditions.

The overall tissue volume decreased for normal tissue to 91% at maximal contraction.

4. Discussion and conclusions

Simulations with a hybrid deformation model were presented to evaluate the capabilities for pathologic tissue simulations of a ventricle model. Three scenarios were investigated. The model representing behavior of normal tissue utilized spring parameters and nonlinear tissue parameters as found in [4, 8]. For simulations of pathologic tissue a patch of $8\times9\times10$ cubic voxel was selected and tissue parameters were adapted to represent necrotic and dilated tissue.

Deformation results show an expected behavior of the elastomechanical ventricular model. Difference in cavity volume, torsion and overall deformation of the elastomechanical ventricular model were recorded.

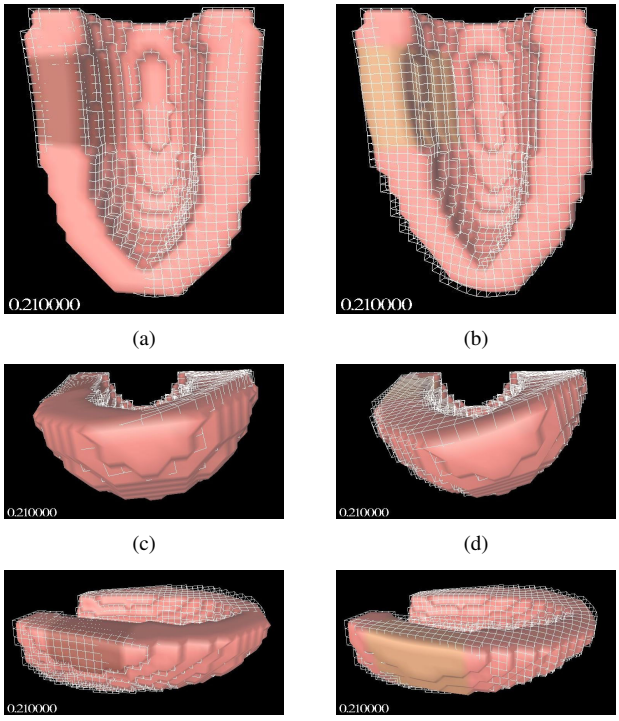

Figure 6. Lateral and basal view of truncated half ellipsoid at maximal deformation for pathologic scenarios. In all pictures the wireframe denotes the deformation with normal tissue, whereas the surface rendering shows pathologic simulations at 0.210 s. The left and right column displays deformation with necrotic patch (a,c,e) and dilated patch (b,d,f), respectively.

Simulations depict that the model is suitable for simulation of pathologic tissue. Parameters have to be set according to required needs.

5. Future work

Future work will be focused on implementing intra-ventricular pressure to extend the capability of the hybrid deformation model. Further emphasis will be set on simulation of patient specific data. MRI scans will be used to set up a patient specific ventricle geometry with corresponding pathologic regions.

References

[1] Noble D, Varghese A, Kohl P, Noble P. Improved guinea-pig ventricular cell model incorporating a diadic space, I_{Kr} and I_{Ks}, and length- and tension-dependend processes. Can J Cardiol Jan. 1998;14(1):123–134.

[2] Henriquez CS, Muzikant AL, Smoak CK. Anisotropy, fiber curvature and bath loading effects on activation in thin and thick cardiac tissue preparations: Simulations in a three-dimensional bidomain model. J Cardiovasc Electrophysiol May 1996;7(5):424–444.

[3] Sachse FB, Glänzel K, Seemann G. Modeling of protein interactions involved in cardiac tension development. Int J Bifurc Chaos 2003;13(12):3561–3578.

[4] Mohr MB, Blümcke LG, Sachse FB, Seemann G, Dössel O. Hybrid deformation model of myocardium. In Proc. CinC, volume 30. 2003; 319–322.

[5] Mohr MB, Blümcke LG, Seemann G, Sachse FB, Dössel O. Volume modeling of myocard deformation using a spring mass system. LNCS 2673 2003;332–339.

[6] Bourguignon D, Cani MP. Controlling anisotropy in mass-spring systems. In Computer Animation and Simulation '00, Proc. 11th Eurographics Workshop, Interlaken, Switzerland, Springer Computer Science. Springer, Aug. 2000; 113–123.

[7] Bathe KJ. Finite Element Procedures. Upper Saddle River, New Jersey: Prentice Hall, 1996. ISBN 0-13-301458-4.

[8] Sachse FB. Modeling of the mammalian heart. Universität Karlsruhe (TH), Institut für Biomedizinische Technik, 2002. Habilitationsschrift.

[9] Greve R. Kontinuumsmechanik. Vorlesungsskript, Fachbereich Mechanik (AG3), TU Darmstadt, 2000.

[10] Miyazaki S, Yasuda T, Yokoi S, Toriwaki J. Modeling and implementation of elastic object manipulation in virtual space. Electronics and Communications in Japan Part 3 Fundamental Electronic Science 1998;1:1919–1926.

[11] Guccione JM. Finite element modeling of ventricular mechanics. In Glass L, Hunter P, McCulloch A (eds.), Theory of Heart. Berlin, Heidelberg, New York: Springer. ISBN 3-540-97483-0, 1991; 121–127.

[12] ANSYS, Inc. ANSYS Theory Reference, 2004.

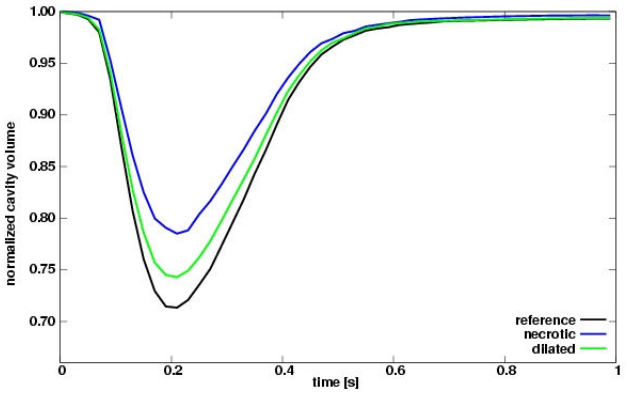

Figure 7. Graph of volume change of cavity volume

Address for correspondence:

Matthias B. Mohr
Institut für Biomedizinische Technik, Universität Karlsruhe (TH)
Kaiserstr. 12 / 76128 Karlsruhe / Germany
tel./fax: ++49-721-608-8035/2789
Matthias.Mohr@ibt.uni-karlsruhe.de